good. It has been assumed that all the ions considered are soluble to an adequate extent in the $BaTiO_3$ which may not necessarily be true.

The minimum concentration of the various dopants needed to prevent the reduction of $BaTiO_3$ is dependent upon the value of x in Equation 1, which, in turn, is a function of the reducing conditions employed. Estimates of x have been made by Arend and co-workers [10, 11] and utilized by Burn and Maher [7] to compute the dopant level needed. The amount of dopant needed exceeds the calculated value if the dopant can exist in more than one oxidation state (e.g. 2+, 3+ and 4+ in the case of Mn) under the conditions of temperature and P_{O_2} employed or if the dopant can occupy more than one type of lattice site (e.g. Mn^{2+} occupying Ba site, while Mn^{2+}, Mn^{3+} and Mn^{4+} can occupy the Ti site).

Based on lattice energy decrease due to the presence of various ions in the $BaTiO_3$ lattice, it was shown that the effectiveness of inhibiting reduction of $BaTiO_3$ in a reducing atmosphere is in the order

$$Mn > Co > Cr > Fe > V > Ga$$

which is in good agreement with experimental results.

References

1. J. M. HERBERT, *Trans. Brit. Ceram. Soc.* **62** (1963) 645.
2. J. M. HERBERT, *Proc. IEE* **112** (1965) 1474.
3. I. BURN, *Amer. Ceram. Soc. Bull.* **57** (1978) 600.
4. *Idem, J. Mater. Soc.* **14** (1979) 2453.
5. A. M. J. H. SAUTER, *Philips Res. Rept. Suppl.* **3** (1974) 46.
6. J. DANIELS, *ibid.* **31** (1978) 505.
7. I. BURN and G. H. MAHER, *J. Mater. Sci.* **10** (1975) 633.
8. N. F. MOTT and M. J. LITTLETON, *Trans. Faraday Soc.* **34** (1938) 485.
9. P. COUFOVA, *Czech. J. Phys.* **B18** (1968) 1038.
10. J. NOVAK and H. AREND, *J. Amer. Ceram. Soc.* **47** (1964) 531.
11. H. AREND and L. KIHLBORG, *ibid.* **52** (1969 63.

Received 2 October
and accepted 5 December 1979

S. B. DESU*
E. C. SUBBARAO
Indian Institute of Technology,
Kanpur 208016,
India

*Present address: 204 Ceramics Building, University of Illinois, Urbana, Illinois 61801, USA.

Eutectic alloys of thorium–niobium and thorium–titanium

Eutectic alloys of niobium–thorium solidify with a rod eutectic morphology, and consequently directionally solidified alloys produce aligned filaments of Nb in a Th matrix. The solid solubility in both phases is quite low and, therefore, such alloys are excellent model systems for studying superconducting properties at superconducting–normal interfaces. In addition, thorium–titanium also forms a eutectic system with very low solid solubility in the constituent phases, so that one has the potential of preparing aligned Nb–Ti filaments by directional solidification from ternary Nb–Ti–Th alloys. Such alloys would provide an

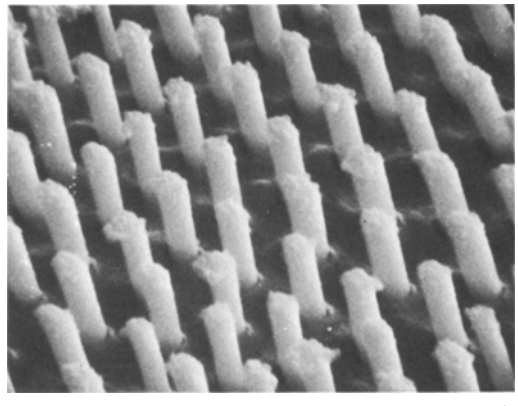

Figure 1 Transverse section of directionally solidified Nb–Th eutectic alloy, deep etched to illustrate aligned structure of Nb filaments. Solidification rate = 45 μm sec^{-1} × 17 200.

0022–2461/80/082115–03$02.30/0

TABLE I Binary eutectic compositions determined by the zone-melting technique

Alloy	Average final zone analysis (wt %)	Range of values in final zone analyses (wt %)	Eutectic values from [3] (wt %)
Nb–Th	7.07	+ 0.08 − 0.04	8
Ti–Th	13.26	+ 0.35 − 0.23	12

excellent model system for studying properties of Nb–Ti filaments similar to those in the currently most popular commercial superconducting wire, Nb–Ti–Cu. This communication reports on an experimental determination of the eutectic composition of the two binary alloys Nb–Th and Ti–Th.

The eutectic compositions were determined by zone-refining alloys rods having compositions near to the expected eutectic compositions. The zone-refining was done by the vertical float zone method at a solidification rate of 1 $\mu m\,sec^{-1}$ using electron-beam heating and a vacuum level of 2×10^{-7} Torr. The solid solidifying from the final zone was examined metallographically to ensure that its structure was fully eutectic. Then, the final solidified zone was chemically analysed and an average value was taken as the eutectic composition. Additional details of the method, plus a discussion of potential errors, have been presented elsewhere [1].

The purity of the starting metal was determined using combustion analysis for C, vacuum fusion analysis for O, N and H, and spark source mass spectroscopy for the remaining elements. The purities with respect to metallic elements were: Th 99.92, Nb 99.98 and Ti 99.94 at %. The sum of the C, O, N and H analyses were: Th 250, Nb 550 and Ti 150 ppm atomic. Detailed analyses are presented elsewhere [2]. In spite of efforts to maintain a very low vacuum level in the zone-refining chamber the Th–Nb alloys often contained a small amount (less than 2 vol %) of ThO_2 dendrites, apparently due to residual oxygen plus pick-up of oxygen by the molten zone. These dendrites were deduced to be ThO_2 because microprobe analysis showed them to contain only Th, and because they charged-up in the scanning electron microscope thereby indicating they were non-conducting.

The experimental results of this study are presented in Table I. The results are averages of two experiments and four analyses on Nb–Th and two experiments and three analyses on Ti–Th. The literature values of Carlson *et al.* [3] were determined by standard phase-diagram techniques and it is seen in Table I that reasonably good agreement is obtained with these values.

Many alloys of Nb–Th have been prepared for studies of their superconducting properties where the filament spacing has been varied by varying the solidification rate. Excellent alignment of Nb filaments has been achieved at solidification rates below 100 $\mu m\,sec^{-1}$, as shown in Fig. 1. However, when the solidification rate was increased into the range of 100 to 200 $\mu m\,sec^{-1}$ a significant colony structure [4] was observed, which is thought to be the result of residual impurities. Analysis of several experiments in the growth rate range of 1 to 5 $\mu m\,sec^{-1}$ yielded the following equation for number of filaments per mm^2, N,

$$N = 20\,000 + 41\,200R$$

where R is the solidification rate in $\mu m\,sec^{-1}$.

Acknowledgements

The authors are indebted to R. J. Hofer and M. J. Tschetter under the direction of R. Bachman for the chemical analyses performed. This research was supported by the US Department of Energy, contract no. W-7405-Eng-82, Office of Basic Energy Sciences, Division of Materials Science (AK-0602).

References

1. T. E. PEDERSEN and J. D. VERHOEVEN, *J. Less-Common metals,* to be published.
2. T. E. PEDERSEN, M.S. Thesis, Iowa State University Library (1980).
3. O. N. CARLSON, J. M. DICKINSON, H. E. LUNT and H. A. WILHELM, *Trans. AIME* **206** (1956) 132.

4. L. M. HOGAN, R. W. KRAFT and F. D. LEMPKEY, in "Advances in Materials Research", Vol. 5, edited by H. Herman (Wiley, New York, 1971) p. 83.

T. E. PEDERSEN*
M. NOACK
J. D. VERHOEVEN
Ames Laboratory-USDOE, and Department of Materials Science and Engineering, Iowa State University, Ames, Iowa 50011, USA

Received 11 December 1979
and accepted 11 January 1980

*Present address: Bendix, Kansas City, Missoui, USA.

Penetration resistance of a magnesium casting alloy

The low density of magnesium alloys has encouraged investigations into their performance as armour materials [1]. Previous work has shown that fracture is a problem, and that one way of avoiding this is to alloy the magnesium to change the crystal structure. An alternative is to support the armour with ductile back-up plates to inhibit brittle failure modes. In either case the function of the armour is to absorb the kinetic energy of the projectile and this requires plastic flow at the highest possible flow stress. Lightweight armours thus require a high ratio of strength to density. The investigation described in this report seeks to assess the influence of microstructural changes on the ballistic performance of a typical magnesium casting alloy.

The alloy chosen was the general purpose casting alloy BS2970 MAG 1 [2] which has the nominal composition in weight per cent, 8% Al, 0.5% Zn, 0.3% Mn and the balance magnesium. The alloys were sand cast into moulds 200 mm by 200 mm, of thickness 18 mm, heavily chilled at one end; they were stress-relieved for 3 h at 260° C after casting. Radiographs showed the castings were very low in porosity.

Mechanical and ballistic tests were carried out on the alloys in three conditions: (a) as-cast and stress-relieved, (b) solution-treated, and (c) aged. The solution treatment involved heating for 8 h at 385° C and 16 h at 420° C followed by an air cool [3]. Ageing was for 1 h at 280° C following the solution treatment.

Stress/strain characteristics were determined using uniaxial compression tests on samples in the three conditions. Ballistic tests involved the use of 4.8 mm diameter conical penetrators with an included angle of 45° at the tip, a maximum tip diameter of 0.015 mm, and a mass of 2.83 g. The details of testing have been described previously [4]. Critical velocities to penetrate targets were determined as the mean of the highest velocity at which the projectile was stopped and the lowest velocity at which penetration was achieved. In some cases a critical velocity for fragment ejection from the rear of the targets, known as discing, was also determined in the same manner.

The stress/strain curves for the alloy in the three conditions are shown in Fig. 1. The strength did not vary a great deal with heat-treatment but the ductility changed markedly. The hardness of the alloy was 66 HV in both the as-cast, stress-relieved and the aged conditions and 58 HV in the solution-treated state. There was a slight variation in properties throughout the castings and the curves of Fig. 1 and the values of hardness represent the mean values determined from a number of tests.

Critical velocities to defeat targets of thicknesses 6.4 and 12.7 mm are given in Table I for each heat-treatment condition. For the thicker targets, it was possible to separate the velocities for fragment ejection and projectile penetration; however, with the thin targets the difference between these critical velocities was less than the error in measurement of the critical velocity. In all cases fragments were ejected from the back of the target, a typical example being that of Fig. 2a. The disced area was of irregular shape although the fracture path tended to follow planes parallel to the surface of the target (Fig. 2b), characteristic of

0022–2461/80/082117–04$02.40/0